Available online at www.sciencedirect.com
SCIENCE DIRECT
Geochimica et Cosmochimica Acta 70 (2006) 3613–3624
Geochimica
www.elsevier.com/locate/gca

A combined FTIR and TPD study on the bulk and surface dehydroxylation and decarbonation of synthetic goethite

Jean-François Boily *, János Szanyi, Andrew R. Felmy

Pacific Northwest National Laboratory, P.O. Box 999, Richland, WA 99352, USA

Received 18 October 2005; accepted in revised form 25 May 2006

Abstract

The thermal dehydroxylation of a goethite–carbonate solid solution was studied with combined Fourier-transform infrared (FTIR)–Temperature programmed desorption (TPD) experiments. The TPD data revealed dehydroxylation peaks involving the intrinsic dehydroxylation of goethite at 560 K and a low temperature peak at 485 K which was shown to be associated to the release of non-stoichiometric water from the goethite bulk and surface. The FTIR and the TPD data of goethite in the absence of adsorbed carbonate species revealed the presence of adventitious carbonate mostly sequestered in the goethite bulk. The release of carbonate was however not only related to the dehydration of goethite but also from the crystallization of hematite at temperatures exceeding 600 K. The relative abundance of surface hydroxyls was shown to change systematically upon goethite dehydroxylation with a preferential stripping of singly-coordinated —OH sites followed by a dramatic change in the dominance of the different surface hydroxyls upon the formation of hematite.

1. Introduction

Interactions between iron oxides and carbonate ions have attracted much attention due to their importance in natural systems (e.g. Oelkers and Schott, 2005). Carbonate complexes on ferric iron oxide surfaces exhibit a diverse speciation scheme and play an important role in the geochemistry of water/rock systems (Zeltner and Anderson, 1988; Wijnja and Schulthess, 2000; Villalobos and Leckie, 2000, 2001; Villalobos et al., 2003; Bargar et al., 2005). Ferric iron (oxy)(hydr)oxides can also form stable solids phases with carbonate at low temperature, including carbonate green rust (Génin et al., 2005) and totally oxidized carbonate green rust (ferric oxyhydroxycarbonate) (Legrand et al., 2004). Goethite–carbonate solid solutions were also identified (Yapp, 1987; Yapp and Poths, 1992, 1993) and have most particularly been useful in paleoclimatic studies for their carbon isotopic composition (e.g. Yapp, 1987; Yapp and Poths, 1990, 1993; Yapp, 2001).

Goethite–carbonate solid solutions have vibrational spectra characteristic of inner-sphere ferric iron–carbonato complexes (Yapp and Poths, 1990) that are similar to adsorbed forms of carbonate on dry goethite (Russell et al., 1975). In spite of its similarity to adsorbed carbonate, bulk carbonate is likely to be more stable than adsorbed forms as it is physically sequestered by the host solid. While it has been proposed to be associated to structural O^{2-} ions in pseudochannels, running along the *c*-axis of goethite (Russell et al., 1975; Yapp, 1987), it is yet not clear whether carbonate solely lies at distinct sites or whether it has a more diverse bulk speciation. For instance, it may be possible that carbonate is associated to non-stoichiometric water in interstices and defects of the host solid. Such forms could be more weakly associated to the solid phase than those forming specific ferric iron–carbonato complexes. Sequential decarbonation reactions can, in this respect, help elucidate the different sources and the relative stabilities of carbonate in the goethite bulk. These can also be used to probe the reactivity of adsorbed carbonate in relation to their bulk-sequestered counterparts.

* Corresponding author. Fax: +1 509 376 3650.
E-mail address: boily@pnl.gov (J.-F. Boily).

0016-7037/$ - see front matter © 2006 Published by Elsevier Inc.
doi:10.1016/j.gca.2006.05.013

In this study, the combined Fourier-transform infrared–Thermal programmed desorption (FTIR–TPD) technique was used to monitor coexisting dehydroxylation and decarbonation reactions during the thermal dehydroxylation of goethite. Carbonate-bearing goethite, which can be characterized as a solid solution of the type α-Fe[$O_{(1-x)}(CO_3)_x$]OH (s) (Yapp, 1987; Yapp and Poths, 1991, 1992, 1993; Yapp, 2001,2003), dehydroxylates via the thermally-induced reaction

$$2\alpha\text{-Fe}[O_{(1-x)}(CO_3)_x]OH(s) \rightarrow \alpha\text{-}Fe_2O_3(s) + H_2O(g) + 2x\ CO_2(g) \quad (1)$$

also liberating CO_2 to its surroundings (e.g. Koch, 1985; Yapp and Poths, 1991, 1992, 1993; Yapp, 2001). While the dehydroxylation mechanisms of goethite have been extensively studied and notably reviewed by Cornell and Schwertmann (2004), little is known on the liberation of occluded forms of carbonate. The FTIR–TPD technique, which enables correlations between decomposition products (e.g. H_2O and CO_2) and the vibrational modes of the transforming material, is particularly useful to follow dehydroxylation and decarbonation reactions in situ over a wide range of temperatures. In addition, by making use of high specific surface area particles, sufficient throughput enables surface-specific reactions to be monitored. In this study, synthetic goethite is used to study dehydroxylation and decarbonation reactions both in the bulk and at surfaces of particles, building upon previous studies which have mostly focused on the bulk dehydroxylation of carbonate-free goethite particles using Differential Thermal Analysis, Constant Rate Thermal Analysis, Thermogravimetric Analysis, Transmission Electron Microscopy, Differential Scanning Calorimetry, Mössbauer Spectroscopy, and X-ray Diffraction (e.g. Schwertmann, 1984; Goñi-Elizalde and García-Clavel, 1988; Pérez-Maqueda et al., 1999; Walter et al., 2001). It also builds upon previous FTIR studies by Ruan et al. (2001, 2002) which have alluded to the presence of adventitious carbonate in the dehydroxylating solid phase of goethite.

2. Materials and methods

2.1. Goethite synthesis

Several goethite preparations were made by converting aqueous suspensions of freshly-precipitated ferrihydrite (pH 12) to goethite in aqueous solutions at 358 K for a period of 48 h. All solutions and suspensions were in stored and prepared in polyethylene or polycarbonate bottles.

A 95 m^2/g carbonate-bearing goethite preparation was made for the FTIR–TPD experiments while all other preparations were made for separate ATR–FTIR measurements. These include one carbonate-free 95 m^2/g goethite preparation and two carbonate-bearing preparations with $N_2(g)$ B.E.T. (Brunauer et al., 1938) specific surface area of 15 m^2/g and 33 m^2/g. All preparations were confirmed to be solely composed of goethite by X-ray powder diffraction (analysis at 0.02°/s).

Both 95 m^2/g goethites were made by the drop-wise titration of a 2.5 mol kg^{-1} NaOH (Aldrich) solution to a vigorously stirred aqueous solution of 0.15 mol kg^{-1} $Fe(NO_3)_3$ (Aldrich) to pH 12 at 293 K. The carbonate-bearing goethite was made in an open atmosphere, starting from a carbonate-bearing ferrihydrite (e.g. Amonette and Rai, 1990), and dialyzed in a polycarbonate beaker for 2 weeks until the conductivity of the filtrate was about 5 times larger than distilled water. The resulting suspension was stored in a polyethylene bottle in contact with the atmosphere. The carbonate-free goethite was made from reagents purged from dissolved CO_2 with dry $N_2(g)$ for a period of 7 days. A 2.5 M NaOH solution was made by diluting a filtered 50% NaOH solution, where the solubility of sodium carbonate is small, into degassed deionized water and further degassed for an additional 7 day period. The synthesis was made under glove box-type conditions in a dry $N_2(g)$ atmosphere and the resulting ferrihydrite was converted to goethite in a water bath at 358 K for 48 h under the same conditions. The carbonate-free goethite suspension was washed by centrifugation using degassed deionized water. While CO_2 could not be strictly eliminated during this last step any adventitious carbonate contamination would have only arose at the surface of the particles and consequently readily desorbed under appropriate degassing conditions. The 15 m^2/g goethite was made following the same procedure as the 95 m^2/g goethite except that ferrihydrite was synthesized at 358 K. The 33 m^2/g goethite was made according to Atkinson et al. (1967).

2.2. FTIR–TPD

Batch-type experiments were carried out to prepare the goethite samples used for the FTIR–TPD experiments. The FTIR–TPD measurements were carried out on the carbonate-bearing 95 m^2/g goethite. One sample was directly taken from the dialyzed goethite suspension in equilibrium with the atmosphere. A second sample was prepared in 0.1 M NaCl (Aldrich, dried at 493 K for 2 h) by adding 2 mM sodium bicarbonate (Aldrich), achieving a carbonate surface density of 1.4 μmol m^{-2} after 24 h of equilibration at pH 6.5 (e.g. Villalobos and Leckie, 2000). The presence of the background electrolyte in this sample was deemed necessary to minimize the formation of outer-sphere/hydrogen-bonded complexes and maximize metal-bonded complexes (Bargar et al., 2005) that would persist in the dried goethite samples used for the FTIR–TPD experiments.

These samples were centrifuged, dried at 358 K for 24 h and ground into powders. A small amount of solid sample (~10 mg) was pressed onto a fine tungsten mesh which was attached onto a copper sample holder assembly. The samples were thereafter heated at a constant rate of 12 K/min from 300 to 880 K under an operating pressure of 10^{-9} Torr. Temperature was measured using a K-type

thermocouple spot-welded to the top center of the tungsten grid and the effluent gases were analysed with a UTI 100 mass spectrometer directly connected to the IR cell through a gate valve. The IR cell is a 2 $\frac{3}{4}$// stainless steel cube equipped with KBr IR windows connected to the mass spectrometer, the gas handling manifold and the pumping station. The IR spectra were collected in transmission mode at 4 cm^{-1} resolution using a Nicolet Magna 750 spectrometer equipped with a MCT detector. Each spectrum was an average of 128 scans. Prior to spectral acquisition, a background spectrum was collected with the sample out of the IR beam.

Band component analysis of the FTIR spectra was carried out by fitting a Gauss–Lorentz function

$$A(\lambda) = e^{-2.30258}\left\{\sum_{1}^{n} x_2 \frac{e^{-x_4^2(\lambda - x_1)^2}}{1 + x_3^2(\lambda - x_1)^2}\right\} \quad (2)$$

where $A(\lambda)$ is the wavenumber-dependent absorbance vector resulting from a linear combination of n bands, λ is the wavenumber (cm^{-1}) and the four x_1, x_2, x_3, and x_4 variables are the adjustable parameters for each individual band. The adjustable parameters were optimized by minimizing the sum-of-squares of the deviations of this model using a Levenberg–Marquardt iteration technique (Marquardt, 1963).

2.3. ATR–FTIR

All goethite samples were analyzed by ATR–FTIR spectroscopy using the thin-film technique (e.g. McQuillan, 2001). An aliquot of the equilibrated suspensions of goethite was transferred on the ATR cell (single-bounce diamond, DuraSampl*IR*) and allowed to evaporate overnight at 293 K in a dry N_2(g) atmosphere. ATR–FTIR spectra were collected every 0.5 h as the suspension evaporated to yield a dry thin film, a process that was confirmed to take about 15–20 h, judging by the time-invariant spectra. The spectra were collected with a Bruker IFS 66/S FTIR spectrometer, operated with a DTGS detector at 4 cm^{-1} resolution, and are the average of 500 scans.

Analyses of deuterated goethite surfaces were also made using the thin-film technique from a goethite (α-FeOOH) suspension in D_2O. This suspension was made by repeated cycles of centrifugation and D_2O washes from an original aqueous suspension. The resulting ATR–FTIR spectra revealed insignificant traces of H_2O in the thin films.

3. Results and discussion

3.1. FTIR spectra of goethite

The FTIR spectrum of carbonate-bearing goethite at 300 K (Fig. 1, top spectrum) exhibits a broad band in the 2600–3800 cm^{-1} region, two sharper bands of lower intensity in the 1600–1800 cm^{-1} region and two other bands in the 700–900 cm^{-1} region. These features are consistent with previously published values for synthetic goethite (Schwarzmann and Sparr, 1969; Parfitt et al., 1975; Rochester and Topham, 1979a,b; Busca et al., 1978; Verdonck et al., 1982; Morterra et al., 1984; Ishikawa et al., 1986; Williams and Guenther, 1996; Weckler and Lutz, 1998; Ruan et al., 2001, 2002; Krehula et al., 2002; Subbanna et al., 2002; Betancur et al., 2004). All bands undergo substantial changes with temperature, as it will be discussed further in Section 3.2.

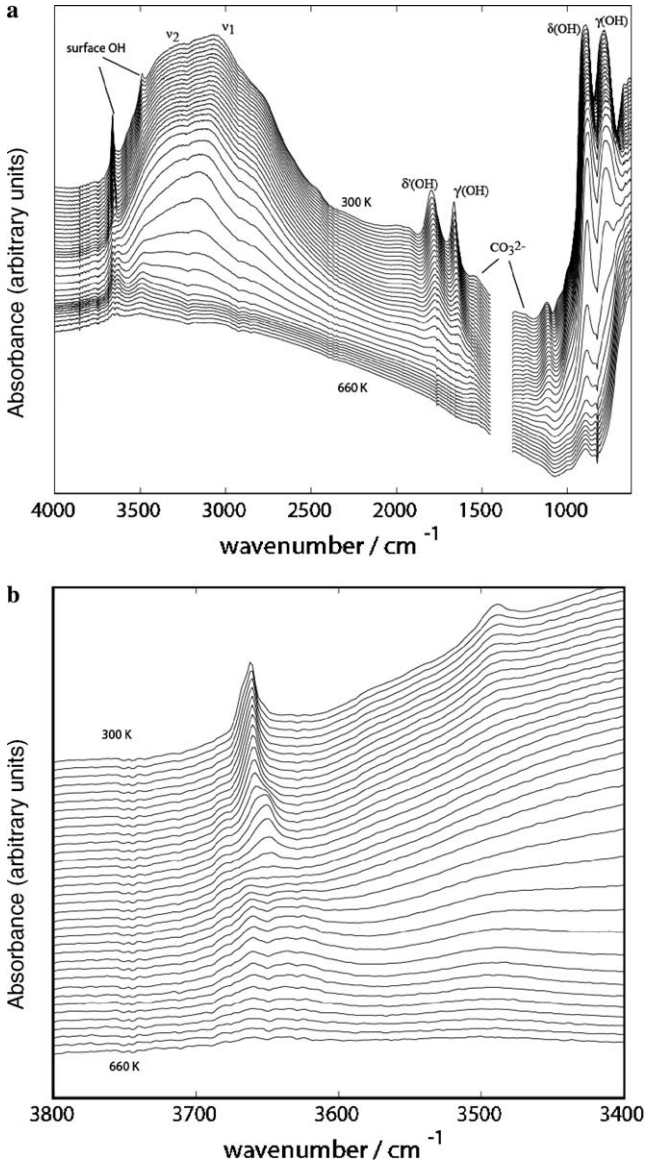

Fig. 1. (a) Transmission FTIR spectra of dried carbonate-bearing 95 m^2/g goethite taken from the FTIR–TPD experiments showing the progressive loss of OH stretches and bends as temperature is increased. The spectra are collected in the 300–660 K range at 10 K intervals. (b) Surface OH stretching region.

3.1.1. OH bending modes

The two sharp bands in the 700–900 cm^{-1} region result from in-plane hydroxyl deformation relative to the vicinal

iron atoms (895 cm^{-1}, δ(OH)) and out-of-plane deformations, parallel to the *c*-axis (792 cm^{-1}, γ(OH)) (Schwertmann et al., 1985; Cambier, 1986a,b). The two other bands in the 1600–1800 cm^{-1} region are, respectively, the first overtone of 895 cm^{-1} hydroxyl bends centered at 1789 cm^{-1}, and a $\delta(OH) + \gamma(OH)$ combination mode centered at 1662 cm^{-1} (Stegmann et al., 1973; Busca et al., 1978; Morterra et al., 1984; Kohler et al., 1997). In comparison, the spectra of Ruan et al. (2002) exhibit some differences which may be explained by differences in goethite sample preparation (e.g. residual moisture, speciation of adventitious carbonate, and residual ferrous iron components from the Ruan et al. (2002) preparation), and the microscopic (vs. transmission) FTIR measurements. Some contributions from the bending vibrations of H_2O in the 1663 cm^{-1} band (e.g. Morterra et al., 1984; Subbanna et al., 2002) are present near the 1635 cm^{-1} region from both bulk and sorbed water molecules (Schwarzmann and Sparr, 1969; Baltrusaitis and Grassian, 2005). In accordance with these claims, ATR–FTIR spectra of our thin film of goethite exposed to D_2O (not shown) essentially preserved the 1663 cm^{-1} band but did result in the isotopic shift of a small component of this band to 1207 cm^{-1}, a result also recently obtained by Baltrusaitis and Grassian (2005).

3.1.2. OH stretching modes

The broad 2600–3800 cm^{-1} band corresponds to hydroxyl stretching vibrations and may be decomposed as O–H stretches due to structural hydroxyls (ν_2 at ~3047 cm^{-1} with a shoulder at 2760 cm^{-1}) and excess (non-stoichiometric) water in the goethite bulk (ν_1 at ~3384 cm^{-1}). The broadness of the OH band arises from a range of hydrogen bonding energies in the goethite bulk. The high frequency regime of this broad OH stretching region (Fig. 1b) includes additional narrow OH stretching bands which have been proposed to arise from isolated surface hydroxyls (e.g. Russell et al., 1974, 1975; Rochester and Topham, 1979a,b; Morterra et al., 1984; Ishikawa et al., 1986). Deuteration of the goethite surface shifted these bands by the expected isotopic ratio (not shown) as previously demonstrated by Parfitt et al. (1975), Rochester and Topham (1979b) and Baltrusaitis and Grassian (2005). Measurements of goethite preparations with specific surface area of 95, 33, and 15 m^2/g (Figs. 2b–e) also revealed a strong effect of surface area on the intensity of these bands, further confirming that these originate from surface OH stretches. Contributions from (bi)carbonate/carbonic acid-type OH stretches are also insignificant as these bands were also present in the spectra of the carbonate-free goethite (Fig. 2c). Finally, it should be noted that a range of hydrogen-bonded surface hydroxyls can also present at the surface and that they are most likely manifested as broad bands that are not as resolvable as the discrete-like bands shown here (e.g. Rochester and Topham, 1979a,b; Baltrusaitis and Grassian, 2005).

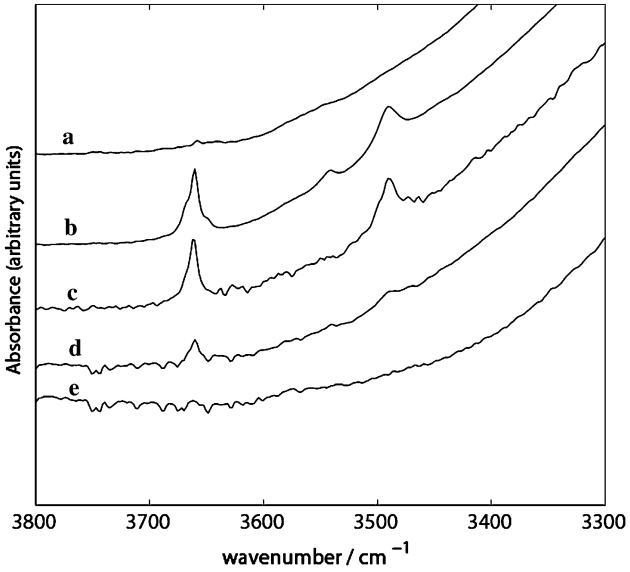

Fig. 2. ATR–FTIR spectra of the surface OH region for four different goethite preparations analyzed using the thin-film technique. (a) carbonate-bearing surface-deuterated 95 m^2/g goethite; (b) carbonate-bearing 95 m^2/g goethite; (c) carbonate-free 95 m^2/g goethite; (d) 33 m^2/g goethite; (e) 15 m^2/g goethite.

3.2. Dehydroxylation

Increasing the temperature from 300 to 660 K (Fig. 1) decreased the intensity of all the bands of goethite, in accordance with previous FTIR dehydroxylation studies (Morterra et al., 1984; Ruan et al., 2001, 2002). The high temperature spectra showed a near-total dehydroxylation of goethite, with attributes similar to those of microporous hematite (Ishikawa et al., 1993).

Several complementary experimental techniques (e.g. DTG–TG, Mössbauer spectroscopy, X-ray diffraction, and transmission electron microscopy) have confirmed goethite to dehydroxylate within this temperature range and to produce hydro-hematite/hematite (Morterra et al., 1984; Schwertmann, 1984; Koch, 1985; Yapp, 1987; Goñi-Elizalde and García-Clavel, 1988; Ford and Bertsch, 1999; Walter et al., 2001; Krehula et al., 2002; Subbanna et al., 2002; Mitov et al., 2002; Przepiera and Przepiera, 2003; Betancur et al., 2004). The transformation of goethite to hematite was also shown to proceed without any intermediate phase, as it can be appreciated by the relatively constant band positions (Fig. 1). This can be explained by a topotactic transformation mechanism arising from the similar anion framework of both phases (Cudennec and Lecerf, 2005). During this transformation water molecules are expelled from the structure, leaving behind a relatively unaffected framework of hexagonally close-packed O^{2-} ions. The Fe atoms are however the ones that migrate to adopt octahedral face sharing coordination and leading the structure to adopt the more condensed crystallographic phase of hematite (Cornell and Schwertmann, 2004; Cudennec and Lecerf, 2005).

In this section, FTIR–TPD measurements are used to follow the progress of the dehydroxylation reactions. Band component analyses were carried out on every spectra to provide a semi-quantitative description of the reactions. We especially focused on the OH stretching region and the Fe–O–H bending overtones and combinations to follow the loss of hydroxyls from the goethite bulk and surface. Given the broadness of the OH stretching region a factor analysis of the spectra was first carried out to estimate the number of factors responsible for the changes over the 300–660 K range, also considering the surface OH stretches (Fig. 1b). The factor indicator function of Malinowski (1977) revealed seven linearly-independent components. Consistent with this result, a 1:1 Gauss–Lorentz analysis (Fig. 3) also required seven individual band components to fit the data, providing support that at least seven different types of OH stretches are required to understand the dehydroxylation chemistry of goethite. The three dominant band components are similar to those obtain in the microscopic FTIR study of Ruan et al. (2002). Our four additional bands arise for surface OH groups which have not yet been explicitly covered in goethite dehydroxylation studies. The fitted band components showed important variations in area over the 36 temperatures studied. While some variations in peak position were also noted, as previously reported by Ruan et al. (2001, 2002), this discussion is focused on the more important variations in band area in tandem with results from the TPD measurements.

3.2.1. Bulk dehydroxylation

The individual band areas of the bulk OH stretches are shown in Fig. 4a. Those of the 3047 and 2760 cm^{-1} bands

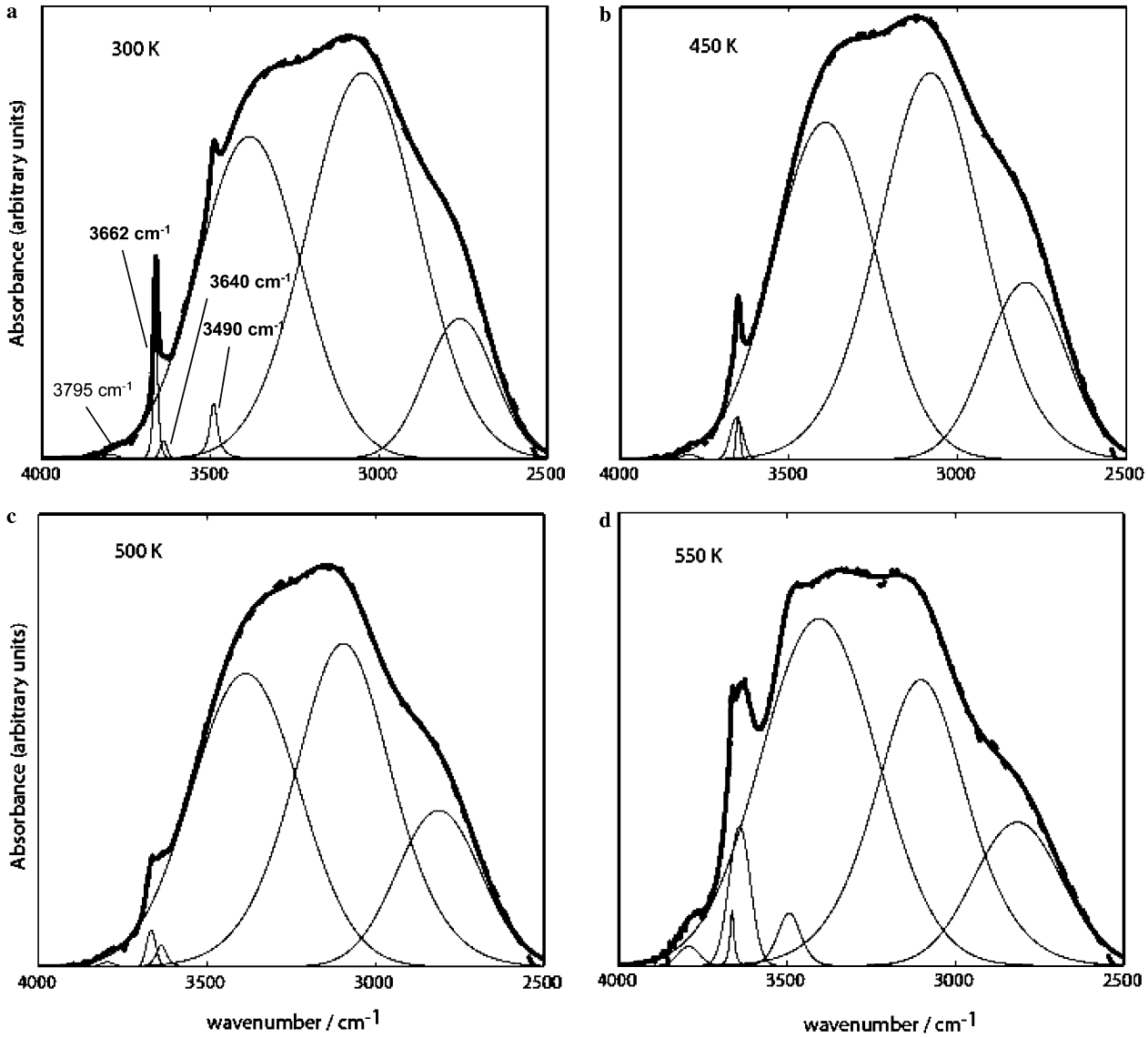

Fig. 3. Gauss–Lorentz band component analysis of the OH stretching region (Fig. 1) at four selected temperatures. The three low energy broad bands correspond to stochiometric hydroxyl and non-stoichiometric water stretches in the goethite bulk. The four high energy discrete-like bands correspond to surface hydroxyls. Thin lines are band components, thick lines are the sum of the components and thick dashed lines are experimental FTIR values.

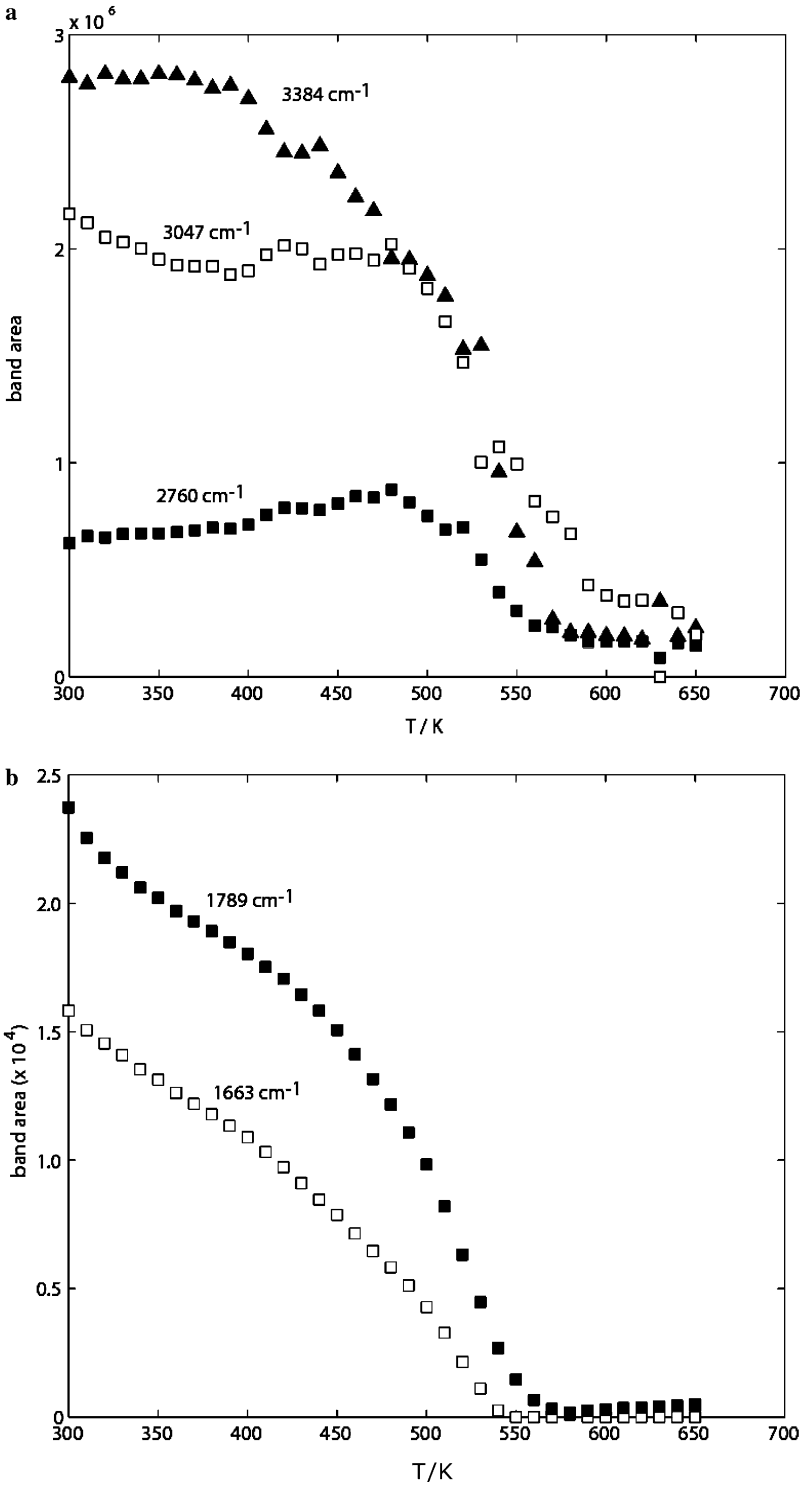

Fig. 4. Individual OH band area obtained from the Gauss–Lorentz band component analysis in the 300–660 K range (Fig. 1) for (a) bulk OH stretches and (b) bending overtones and combinations.

are relatively constant to 475 K, while those of the 3384 cm^{-1} band are initially constant to 375 K and decrease steeply at higher temperatures. The pronounced decrease of the 3384 cm^{-1} band is taken as evidence for a preferential dehydration of non-stoichiometric bulk and surface water over structural OH. Above 475 K structural dehydroxylation reactions are important, as seen by the decreasing 3047 and 2760 cm^{-1} bands, which level off to relatively low-lying values at temperatures above ~600 K. These high temperature bands are attributed to the presence of residual hydroxyls and water in the resulting hematite (Morterra et al., 1984; Ruan et al., 2001, 2002).

The transformation of goethite to hematite is also reflected in the bending modes, as shown in Fig. 4b. While band analysis could not be applied to the δ(OH) and γ(OH) modes due to difficulties with the steeply increasing baseline at wavenumbers ~1000 cm^{-1}, the band areas of the bending overtones, the combination modes and non-stoichiometric water were used to illustrate these effects. In contrast to the two dominant structural OH stretches, the δ'(OH) and δ(OH) + γ(OH) bands decreased throughout the 300–475 K range. Part of the explanation for this important difference lies in contributions from non-stoichiometric bulk water and surface ≡Fe–O–H bends (Morterra et al., 1984), as it will be discussed in the following section. These bands completely disappeared in the 550–575 K range, a result also consistent with the microscopic FTIR measurements of Ruan et al. (2002). Bulk dehydroxylation reactions are however manifested above 475 K where the decrease in band areas, just like in the 3047 and 2760 cm^{-1} bands, are strongly affected by increased temperatures, again underscoring an important release of hydroxyls/water from the solid.

The release of OH from goethite is most particularly recovered in the TPD measurements (Fig. 5). The TPD trace shows a marginal release of H_2O below ~400 K, followed by a marked increase above this value which is manifested in two dominant dehydration/dehydroxylation peaks at 485 and 560 K. In comparison, the temperature of complete transformation was shown to be in the 560–620 K range (Schwertmann, 1984) but was strongly dependent on the intrinsic differences of the starting material, such as sequestered water content, specific surface area, and crystallinity (e.g. Schwertmann, 1984; Goñi-Elizalde and García-Clavel, 1988; Ford and Bertsch, 1999; Walter et al., 2001; Cornell and Schwertmann, 2004). Our 560 K peak lies in the lower part of this range and is associated to the steeply decreasing band areas of the 3047 and 2760 cm^{-1} bands (Fig. 4a), confirming that it arises from the bulk dehydroxylation of goethite. As no other peak is found above this temperature the TPD trace is not characteristic of the well-known DTA double dehydroxylation peak (Derie et al., 1976; Schwertmann, 1984; Walter et al., 2001) but is rather more consistent with a single dehydroxylation event, characteristic of high specific surface area goethite particles, as it was recently discussed by Walter et al. (2001). Our low temperature TPD peak at 485 K occurs, on the other hand, in the same temperature range of the decreasing area of the 3384 cm^{-1} band and consequently arises from the evacuation of non-stoichiometric water molecules from the goethite bulk and, as it will be discussed in the following section, from the goethite surface.

3.2.2. Surface de- and re-hydroxylation

The high energy discrete OH stretches undergo important changes during the dehydroxylation of goethite, indicating that the dehydroxylation of goethite also affects the concentrations of surface functional groups (Fig. 1b). The areas of the dominant low temperature 3491 and 3662 cm^{-1} bands (Fig. 6) decreased by no more than ~2/3rd of their 300 K values in the 300–390 K range. Above this range the 3491 cm^{-1} band areas however decreased to ~475 K while those of the 3662 cm^{-1} band only gradually decreased. As the disappearance of the 3491 cm^{-1} band coincides with the onset of the first TPD

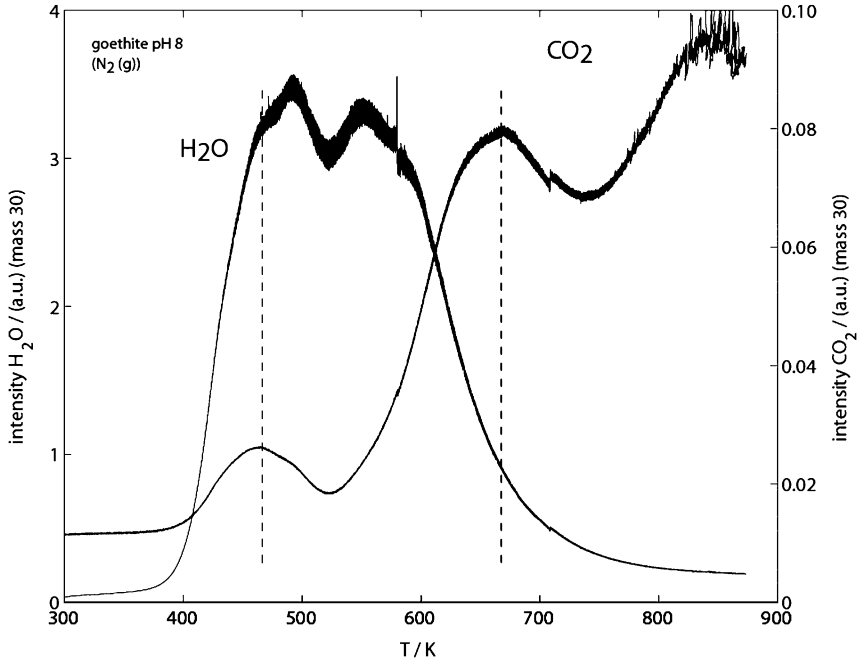

Fig. 5. TPD data for H_2O (left ordinate axis) and CO_2 (right ordinate axis) in the carbonate-bearing 95 m^2/g goethite (pH 6.5, no NaCl) as a function of temperature. Vertical dashed lines note the two decarbonation maxima in relation to the dehydroxylation trace.

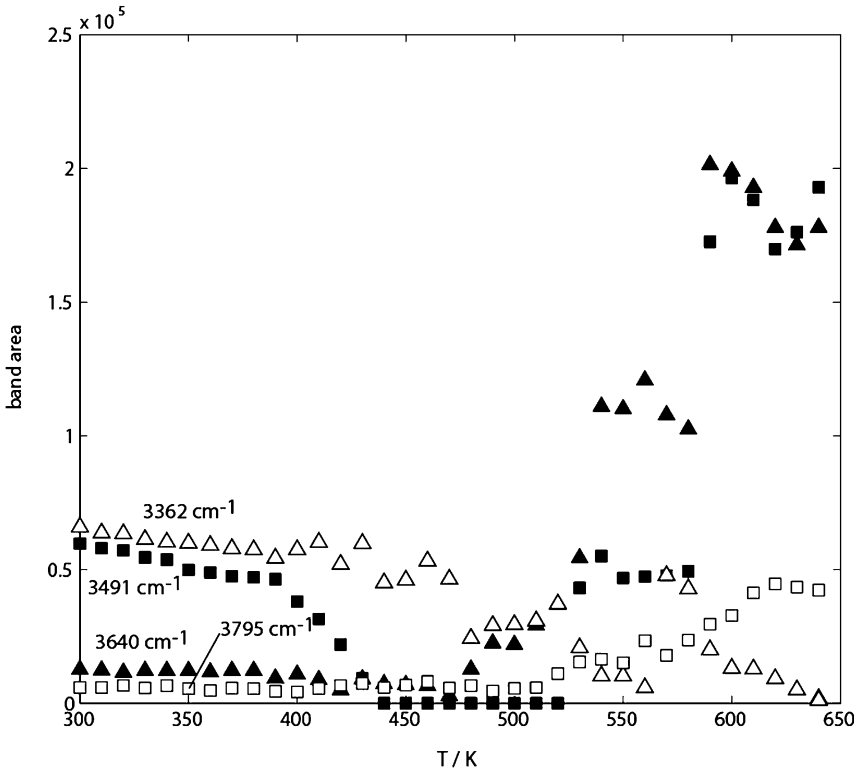

Fig. 6. Individual OH band area obtained from the Gauss–Lorentz band component analysis in the 300–660 K range for the surface OH stretches (Fig. 1).

H_2O desorption event (Fig. 5) we propose that these data be taken as evidence for a preferential stripping of a relatively weakly-bound OH group. This interpretation also concurs with a previous assignment of the 3491 cm^{-1} band to singly-coordinated –OH groups (Russell et al., 1975), which are expected to be less strongly bound to underlying Fe atoms than the doubly- ($\equiv Fe_2OH$; μ-OH) and triply-coordinated ($\equiv Fe_3OH$; μ_3-OH) surface hydroxyls (e.g. Hiemstra et al., 1996). The trend seen in the 3491 cm^{-1} band is also paralleled in the $\delta'(OH)$ and $\delta(OH) + \gamma(OH)$ modes below ~450 K, indicating a substantial loss of Fe–O–H bending modes due to the dehydration of the surface, a process that can be illustrated by the reaction (e.g. Morterra et al., 1984):

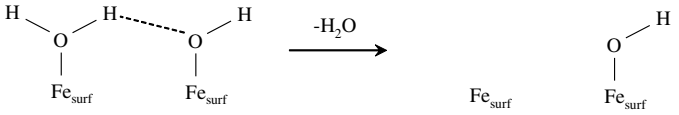

(3)

where Fe_{surf} is a Fe(III) atom located at the surface.

Above 475 K the freshly-dehydroxylated goethite retains a variety of surface hydroxyls up to at least 660 K. These FTIR can data thereby not support previous claims for a sequence of preferential stripping of surface sites in the order –OH > μ-OH > μ_3-OH (Ford and Bertsch, 1999), but rather reveal a gradual change in the surface speciation of the transforming phase. In fact, the aforementioned 3491 cm^{-1} band, which disappeared below 475 K, reappeared on the newly-formed hematite solid above 525 K. At the same time the 3640 cm^{-1} band, assigned to μ-OH by Parfitt et al. (1975), increased substantially and reached similar magnitudes as the 3491 cm^{-1} band at high temperature (Fig. 6). As a whole, these important changes reflect substantial changes in the surface chemistry of the particles during the conversion of goethite to hematite.

3.3. Decarbonation

In addition to the bulk and surface dehydroxylation reactions discussed in the preceding sections the FTIR–TPD experiments provide evidence for the presence of carbonate in the goethite structure. The FTIR spectra of goethite (Fig. 1) exhibited weak bands at 1550 and 1320 cm^{-1} which are similar to C–O stretches from carbonate adsorbed on dry goethite (Fig. 7) and in previous studies (Russell et al., 1975; Rochester and Topham, 1979a,b). These values are similar those obtained by Baltrusaitis and Grassian (2005) on hematite in high relative humidity conditions.

Time-resolved ATR–FTIR measurements of a thin-film of the goethite–carbonate solid solution in $N_2(g)$ atmosphere (Fig. 7) showed a gradual decrease of only these C–O stretches resulting from the desorption of carbonate from the particle surfaces; all other bands in the 500–4000 cm^{-1} range remained largely unperturbed. Residual C–O band components however remained even after several days of exposure to the $N_2(g)$ atmosphere in the ATR–FTIR set-up, and in an overnight evacuation period at 353 K in 10^{-9} Torr in the FTIR–TPD

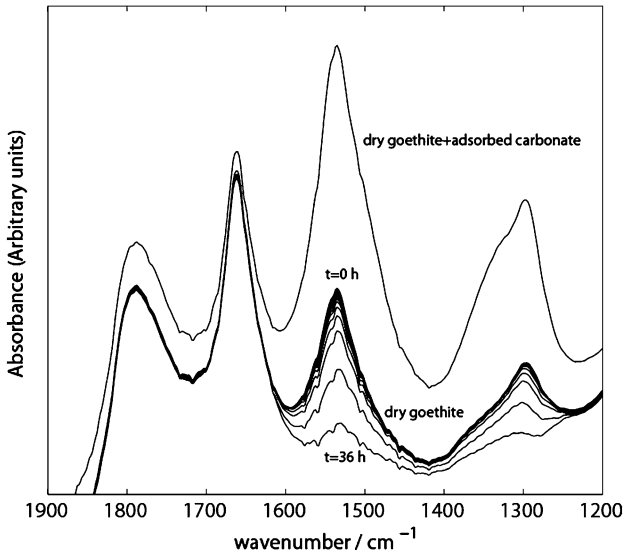

Fig. 7. Spectroscopic evidence for the presence of adsorbed carbonate on the carbonate-bearing 95 m^2/g goethite. Top: ATR–FTIR spectrum of dry goethite with 1.4 μmol m^{-2} adsorbed carbonate. Bottom: selected ATR–FTIR spectra of dry goethite (pH 6.5, no NaCl) at 0.5 h intervals showing a progressive decrease of only the C–O stretches as carbonate desorbs from the goethite surface in a dry N_2(g) atmosphere.

set-up, providing evidence for a resilient fraction of carbonate.

Bands at roughly similar positions as those mentioned here were also noted in naturally-occurring inorganic carbon-bearing goethites and were suggested to arise from sequestered carbonate (Yapp and Poths, 1990). This was confirmed by goethite dehydroxylation studies showing up to ~4% (wt/wt) of occluded forms of CO_2 (Koch, 1985; Yapp and Poths, 1991, 1993; Yapp, 2001). More recently Ruan et al. (2001, 2002) reported residual bands at 1531 and 1287 cm^{-1} resulting from a goethite synthesis procedure involving the oxidation of ferrous iron in the presence of a bicarbonate buffer. While it is not clear whether carbonate sits at structural O^{2-} sites (Russell et al., 1975; Yapp, 1987), coordinated to oxygen vacancies and/or in defects, the important split in these bands, in comparison to the 1430/1375 cm^{-1} bands of CO_3^{2-} in D_{3h} symmetry (Davis and Oliver, 1972; Oliver and Davis, 1973), suggest the formation of inner-sphere ferric iron–carbonato complexes. The 130 cm^{-1} band separation is also consistent with literature values of inner-sphere carbonate surface complexes (Bargar et al., 1999, 2005; Wijnja and Schulthess, 2001; Villalobos and Leckie, 2001) and has been interpreted both as monodentate binuclear (Hiemstra et al., 2004; Bargar et al., 2005) and as monodentate mononuclear complexes (Wijnja and Schulthess, 2001). Coupled experimental-solid state computational efforts along these lines are currently under way in our group to provide further insight into the coordination environment of occluded carbonate.

The experimental evidence provided in this study, which will also assist our ongoing computational efforts, reveals two distinct sources of carbonate through decarbonation events at 485 and 675 K (Fig. 5). While differences in coordination (e.g. mononuclear vs. binuclear) could be used to explain these two events, the relatively constant positions of the C–O stretches in the 300–660 K range points to one dominant coordination scheme. As the first decarbonation event coincides with the first dehydration peak, we propose that it arises from the release of carbonate associated to non-stoichiometric surface and bulk water. On the other hand, as the second event occurs ~100 K above the second dehydroxylation event, we propose that it is associated to a more resilient fraction of carbonate in direct coordination to the structural components of goethite. In this section the release of carbonate is discussed in this context, partially building upon previously-proposed mechanisms

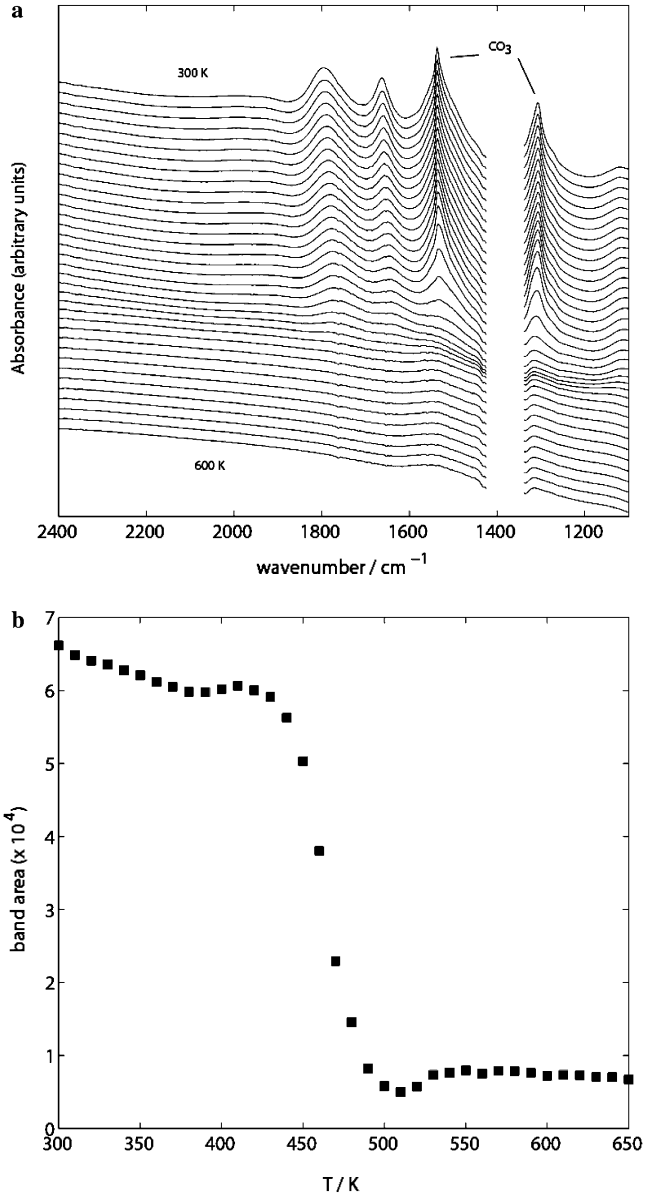

Fig. 8. FTIR measurements of dry goethite with 1.4 μmol m^{-2} adsorbed carbonate on the carbonate-bearing 95 m^2/g goethite. (a) Transmission FTIR spectra in the TPD experiments in the 300–660 K range. (b) Area of the 1530 cm^{-1} band as a function of temperature.

for the dehydroxylation of goethite (Naono and Fujuwara, 1980; Rendon et al., 1983; Goñi-Elizalde and García-Clavel, 1988; Walter et al., 2001; Ruan et al., 2002).

3.3.1. Surface decarbonation

In order to confirm that the first decarbonation event is associated to non-structural carbonate a goethite sample with adsorbed carbonate was studied with FTIR–TPD (Fig. 8a). The low temperature FTIR spectra are identical to those of the goethite-carbonate solid solution but with enhanced band intensities at 1520 and 1300 cm^{-1}, just as in Fig. 7, underscoring a metal-bonded carbonate surface complex of distorted geometry. An analysis of the important 1500 cm^{-1} band showed a marked decrease in band area in the 400–500 K range (Fig. 8b), with a desorption edge 50–100 K below the bulk dehydroxylation of goethite (Figs. 4 and 5). It is interesting to note that this region also coincides with the important loss of surface OH groups (Fig. 6), further showing that this temperature range is associated to desorption reactions. Moreover, as important quantities of carbonate are still adsorbed after the total desorption of the singly-coordinated sites (Fig. 6) these data may be indicating that the inner-sphere ferric iron–carbonato surface complexes can also involve other types of surface functional groups (e.g. μ-O, μ_3-O). This is an important possibility that warrants further investigations, especially along the lines recently explored by Hiemstra et al. (2004).

These results are also paralleled in the TPD data (Fig. 9), showing a remarkable increase in only the 475 K decarbonation event relative to the sample in the absence of adsorbed carbonate (Fig. 5). This event also coincides with the inflection point of the steeply decreasing C–O stretch band areas (Fig. 8b), again confirming that it is associated with surface-bound carbonate and, as shown in the previous sections, with non-structural forms of bulk carbonate associated with non-stoichiometric water. As the second decarbonation event is left unperturbed it can be confirmed that it solely arises from structural forms of carbonate, as it will be discussed in the following section.

3.3.2. Bulk decarbonation

The second decarbonation event takes place ~100 K above the 560 K dehydroxylation of goethite (Fig. 9). As previously stated, this important offset suggests that this decarbonation event is not a direct consequence of dehydroxylation. From the collective evidence of several dehydroxylation studies, it is rather related to the formation of the more confining structure of hematite (Yapp and Poths, 1993). Previous studies on the thermal conversion of goethite into hematite (e.g. Walter et al., 2001; Ruan et al., 2002) showed that water molecules are first liberated via micropores running along of *c*-axis of the goethite bulk and that the newly-formed hematite phase keeps a needle/lath-like appearance up to ~625–700 K. During this stage hematite possesses micropores of about 0.8–1.4 nm in diameter through which both water vapour and CO_2 are expelled from the solid phase. While the dehydroxylation reactions tail off above this temperature range decarbonation reactions involving a resilient fraction of carbonate can proceed to higher temperatures as the solid phase sinters internally to produce closed spherical

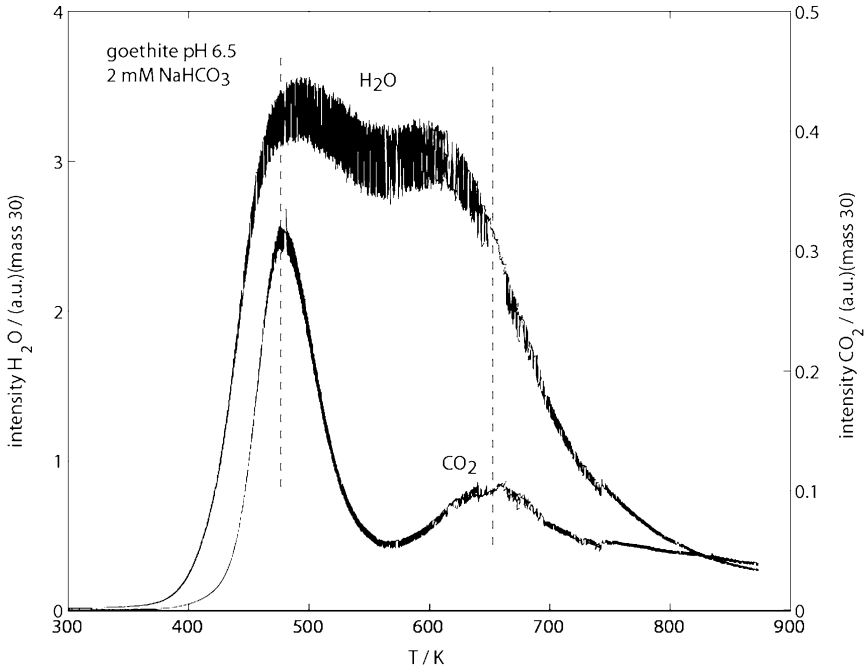

Fig. 9. TPD data for H_2O (left ordinate axis) and CO_2 (right ordinate axis) in the carbonate-bearing 95 m^2/g goethite (pH 6.5, 0.1 M NaCl) sample with 1.4 μmol m^{-2} adsorbed carbonate. Vertical dashed lines note the two decarbonation maxima in relation to the dehydroxylation trace.

mesopores (Naono and Fujuwara, 1980; Rendon et al., 1983). The solids ultimately become more compact, eliminating these mesopores and further expelling occluded forms of carbonate, leaving behind the more compact crystallographic unit of hematite as the final solid phase (Goñi-Elizalde and García-Clavel, 1988; Yapp and Poths, 1993). As the TPD measurements revealed traces of continuously expelled CO_2 at these elevated temperatures, it must be concluded that hematite also contains residual forms of occluded carbonate.

4. Conclusions

The thermal dehydroxylation of high specific surface area synthetic goethite gives rise to a double dehydroxylation peak shifted to lower temperatures, relative to previous DTA measurements. The low temperature peak corresponds to desorbing surface-bound and bulk-sequestered water molecules, while the higher temperature peak is intrinsic to a single dehydroxylation event characteristic of high surface area goethite particles. Dehydroxylation correlates with a decrease in non-stoichiometric OH stretches at the low temperature event and in the stoichiometric OH stretches at the high temperature event. Surface hydroxyl groups ascribed to singly-coordinated –OH groups preferentially desorb from the goethite surface at 475 K, coinciding with the onset of dehydroxylation.

The conversion of goethite to hematite also releases surface- and bulk-bound carbonate originating from the synthesis and suspension storage conditions. While surface and bulk carbonate species have very similar binding modes, the surface-bound carbonate desorbs before bulk dehydroxylation. Carbonate remains associated to hematite but is gradually expelled with increased temperatures.

Acknowledgments

The authors thank two anonymous reviewers and J. Schott for their highly insightful comments. This work was supported by the US Department of Energy, Office of Basic Energy Sciences, Geosciences, Research Program. A portion of the research was performed in the Environmental Molecular Sciences Laboratory, a national scientific user facility sponsored by the Department of Energy's Office of Biological and Environmental Research and located at Pacific Northwest National Laboratory. Pacific Northwest National Laboratory is operated by Battelle Memorial Institute for the U.S. Department of Energy under Contract DE-AC06-76RLO 1830.

Associate editor: Jacques Schott

References

Amonette, J.E., Rai, D., 1990. Identification of noncrystalline $(Fe,Cr)(OH)_3$ by infrared spectroscopy. *Clay Clay Min.* **38**, 129–136.

Atkinson, R.J., Posner, A.M., Quirk, J.P., 1967. Adsoprtion of potential-determining ions at the ferric oxide-aqueous electrolyte interface. *J. Phys. Chem.* **71**, 550–558.

Baltrusaitis, J., Grassian, V.H., 2005. Surface reactions of carbon dioxide at the adsorbed water–iron oxide interface. *J. Phys. Chem. B* **109**, 12227–12230.

Bargar, J.R., Kubicki, J.D., Reitmeyer, R., Davis, J.A., 2005. ATR–FTIR spectroscopic characterization of coexisting carbonate surface complexes on hematite. *Geochim. Cosmochim. Acta* **69**, 1527–1542.

Bargar, J.R., Reitmeyer, R., Davis, J.A., 1999. Spectroscopic confirmation of uranium(VI)-carbonato adsorption complexes on hematite. *Environ. Sci. Technol.* **33**, 2481–2484.

Betancur, J.D., Carrero, C.A., Geneche, J.M., Goya, G.F., 2004. The effect of water content on the magnetic and structural properties of goethite. *J. Alloys Comp.* **369**, 247–251.

Brunauer, S., Emmett, P.H., Teller, E., 1938. Adsorption of gases in multimolecular layers. *Am. Chem. Soc. J.* **60**, 309–319.

Busca, G., Cotena, N., Rossi, P.F., 1978. Infrared spectroscopic study of micronized goethite. *Mat. Chem.* **3**, 271–284.

Cambier, P., 1986a. Infrared study of goethite or varying crystallinity and particle size 1. Interpretation of OH and lattice vibration frequencies. *Clay Min.* **21**, 191–200.

Cambier, P., 1986b. Infrared study of goethites of varying crystallinity and particle size 2. Crystallographic and morphological changes in series of synthetic goethites. *Clay Min.* **21**, 201–210.

Cudennec, Y., Lecerf, A., 2005. Topotactic transformations of goethite and lepidocrocite into hematite and maghemite. *Solid State Sci.* **7**, 520–529.

Cornell, R.M., Schwertmann, U., 2004. *The Iron Oxides*, second ed. Wiley-VCH Verlag.

Davis, J.A., Oliver, B.G., 1972. A vibrational spectroscopic study of the species presence in the CO_2–H_2O system. *J. Sol. Chem.* **1**, 329–339.

Derie, R., Ghodsi, M., Calvo-Roche, C.J., 1976. DTA study of dehydration of synthetic goethite α-FeOOH. *Therm. Anal.* **9**, 435–440.

Ford, R.G., Bertsch, P.M., 1999. Distinguishing between surface and bulk dehydration–dehydroxylation reactions in synthetic goethites by high-resolution thermogravimetric analysis. *Clay Clay Min.* **47**, 329–337.

Génin, J.-M.R., Aïssa, R., Géin, A., Abdelmoula, M., Benali, O., Ernstsen, V., Ona-Nguema, G., Upadhyay, C., Ruby, C., 2005. Fougerite and Fe^{II-III} hydroxycarbonate green rust; ordering, deprotonatino and/or cation substitution; structure of hydrotalcite-like compounds and mythis ferrosic hydroxide $Fe(OH)_{(2+x)}$. *Solid State Sci.* **7**, 545–572.

Goñi-Elizalde, S., García-Clavel, Ma.E., 1988. Themal behaviour in air of iron oxyhydroxides obtained from the method of homogeneous precipitation. Part I. Goethite samples of varying crystallinity. *Thermochim. Acta.* **124**, 359–369.

Hiemstra, T., Rahnemaie, R., van Riemsdijk, W.H., 2004. Surface complexation of carbonate on goethite: IR spectroscopy, structure and charge distribution. *J. Coll. Interface Sci.* **278**, 282–290.

Hiemstra, T., Venema, P., van Riemsdijk, W.H., 1996. Intrinsic proton affinity of reactive surface groups of metal (hydr)oxides: the bond valence principle. *J. Coll. Interface Sci.* **184**, 680–692.

Ishikawa, T., Nitta, S., Kondo, S., 1986. Fourier-transform infrared spectroscopy of colloidal α-, β- and γ-ferric oxide hydroxides. *J. Chem. Soc. Faract Trans. I.* **82**, 2401–2410.

Ishikawa, T., Cai, W.Y., Kandori, K., 1993. Adsorption of molecules onto microporous hematite. *Langmuir* **9**, 1125–1128.

Koch, Chr.J.W., 1985. Differential thermal analysis—evolved gas analysis of synthetic goethite. *Thermochim. Acta* **95**, 395–400.

Kohler, T., Armbruster, T., Libowitzky, E., 1997. Hydrogen bonding and Jahn-Teller distortion inn groutite, α-MnOOH, and manganite, γ-MnOOH, and their relations to the manganese dioxides ramsdellite and pyrolusite. *J. Solid State Chem.* **133**, 486–500.

Krehula, S., Popović, Musić, S., 2002. Synthesis of acicular α-FeOOH particles at a very high pH. *Mater. Lett.* **54**, 108–113.

Legrand, L., Mazerolles, L., Chausse, A., 2004. The oxidation of carbonate green rust into ferric phases: solid-state reaction or

transformation via solution. *Geochim. Cosmochim. Acta.* **68**, 3497–3507.

Malinowski, E.R., 1977. Determination of the number of factors and the experimental error in a data matrix. *Anal. Chim.* **49**, 612–617.

Marquardt, D.W., 1963. An algorithm for least-square estimates of nonlinear parameters. *SIAM J. Opt.* **11**, 431–441.

McQuillan, A.J., 2001. Probing solid-solution interfacial chemistry with ATR-IR spectroscopy of particle films. *Adv. Mat.* **13**, 1034.

Mitov, I., Paneva, D., Kunev, B., 2002. Comparative study of the thermal decomposition of iron oxyhydroxides. *Thermochim. Acta.* **386**, 179–188.

Morterra, C., Chiorino, A., Borello, E., 1984. An IR spectroscopic characterization of α-FeOOH (goethite). *Mat. Chem. Phys.* **10**, 119–138.

Naono, H., Fujuwara, R., 1980. Micropore formation due to thermal-decomposition of acicular microcrystals of α-FeOOH. *J. Coll. Interface. Sci.* **73**, 406–415.

Oelkers, E.H., Schott, J., 2005. Geochemical aspects of CO_2 sequestration. *Chem. Geol.* **217**, 183–186.

Oliver, B.G., Davis, AA.R., 1973. Vibrational spectroscopic studies of aqueous alkali metal bicarbonate and carbonate solutions. *Can. J. Chem.* **51**, 698–702.

Parfitt, R.L., Russell, J.D., Farmer, V.C., 1975. Confirmation of surface-structures of goethite (α-FeOOH) and phosphated goethite by infrared spectroscopy. *J. Chem. Soc. Farad. Trans. I.* **72**, 1082–1087.

Pérez-Maqueda, L.A., Criado, J.M., Real, C., Šubrt, J., Bohàcek, J., 1999. Use of constant rate thermal analysis (CRTA) for controlling the texture of hematite obtained from the thermal decomposition of goethite. *J. Mater. Chem.* **9**, 1839–1845.

Przepiera, K., Przepiera, A., 2003. Thermal transformations of selected transition metals oxyhydroxides. *J. Therm. Anal. Cal.* **74**, 659–666.

Rochester, C.H., Topham, S.A., 1979a. Infrared studies of the adsorption of probe molecules onto the surface of goethite. *J. Chem. Soc. Farad Trans.* **75**, 1259–1267.

Rochester, C.H., Topham, S.A., 1979b. Infrared study of surface hydroxyl-groups on goethite. *J. Chem. Soc. Farad Trans.* **75**, 591–602.

Rendon, J.L., Cornejo, J., Dearambarry, P., Serna, C.J., 1983. Pore structure of thermally treated goethite (α-FeOOH). *J. Coll. Interface Sci.* **92**, 508–516.

Ruan, H.D., Frost, R.L., Kloprogge, J.T., Duong, L., 2002. Infrared spectroscopy of goethite dehydroxylation: III. FT-IR microscopy of in situ study of the thermal transformation of goethite to hematite. *Spectrochim. Acta A* **58**, 967–981.

Ruan, H.D., Frost, R.L., Kloprogge, J.T., 2001. The behaviour of hydroxyl units of synthetic goethite and its dehydroxylated product hematite. *Spectrochim. Acta. A* **57**, 2575–2586.

Russell, J.D., Parfitt, R.L., Fraser, A.R., Farmer, V.C., 1974. Surface-structures of gibbsite goethite and phosphated goethite. *Nature* **248**, 220–221.

Russell, J.D., Paterson, E., Fraser, A.R., Farmer, V.C., 1975. Adsorption of carbon dioxide on goethite (α-FeOOH) surfaces, and its implications for anion adsorption. *J. Chem. Soc. Farad Trans. I* **71**, 1623–1630.

Schwarzmann, E., Sparr, H., 1969. Die Wasserstoffbrückenbindung in Hydroxiden und Diasporstruktur. *Z. Naturforch. B* **216**, 8–11.

Schwertmann, U., 1984. The double dehydroxylation peak of goethite. *Thermochim. Acta* **78**, 39–46.

Schwertmann, U., Cambier, P., Murad, E., 1985. Properties of goethites of varying crystallinity. *Clay Clay Min.* **33**, 369–378.

Stegmann, M.C., Vivien, D., Mazières, C., 1973. Etude des modes de vibration infrarouge dans les oxyhydroxydes d'aluminium boehmite et diaspore. *Spectrochim. Acta* **29**, 1653–1663.

Subbanna, G.N., Sudakar, C., Kutty, T.R.N., 2002. Precipitation of acicular hydrogoethite (α-$FeOOH{\cdot}xH_2O$; $0.1 < x < 0.22$) using morphology controlling cationic additives. *Mat. Chem. Phys.* **78**, 43–50.

Verdonck, L., Hoste, S., Roelandt, F.F., Vanderkelen, G.P., 1982. Normal coordinate analysis of α-FeOOH—A molecular approach. *J. Mol. Struct.* **79**, 273–279.

Villalobos, M., Trotz, M.A., Leckie, J.O., 2003. Variability in goethite surface site density: evidence from proton and carbonate sorption. *J. Coll. Interface Sci.* **268**, 273–287.

Villalobos, M., Leckie, J.O., 2001. Surface complexation modeling and FTIR study of carbonate adsorption to goethite. *J. Coll. Interface Sci.* **235**, 15–32.

Villalobos, M., Leckie, J.O., 2000. Carbonate adsorption on goethite under closed and open CO_2 conditions. *Geochim. Cosmochim. Acta* **64**, 3787–3802.

Walter, D., Buxbaum, G., Laqua, A., 2001. The mechanism of the thermal transformation from goethite to hematite. *J. Therm. Anal. Cal.* **63**, 733–748.

Weckler, B., Lutz, H.D., 1998. Lattice vibration spectra. Part XCV. Infrared spectroscopic studies on the iron oxide hydroxides goethite (α), akaganéite (β), lepidocrocite (γ), and ferroxyhite (δ). *Eur. J. Solid State Inorg. Chem.* **35**, 531–544.

Wijnja, H., Schulthess, 2001. Carbonate adsorption mechanism on goethite studied with ATR–FTIR, DRIFT, and proton coadsorption measurements. *Soil Sci. Soc. Am. J.* **65**, 324–330.

Wijnja, H., Schulthess, C.P., 2000. Interaction of carbonate and organic anions with sulfate and selenate adsorption on an aluminum oxide. *Soil Sci. Soc. Am. J.* **64**, 898–908.

Williams, Q., Guenther, L., 1996. Pressure-induced changes in the bonding and orientation of hydrogen in FeOOH-goethite. *Solid State Comm.* **100**, 105–109.

Yapp, C.J., 1987. A possible goethite-iron(III) carbonate solid solution and the determination of CO_2 partial pressures in low temperature geologic systems. *Chem. Geol.* **64**, 25–268.

Yapp, C.J., 2001. Mixing of CO_2 in surficial environments as recorded by the concentration and $\delta^{13}C$ values of the $Fe(CO_3)OH$ component in goethite. *Geochim. Cosmochim. Acta* **65**, 4115–4130.

Yapp, C.J., 2003. A model for $^{18}O/^{16}O$ variations in CO_2 evolved from goethite during the solid-state α-FeOOH to α-Fe_2O_3 phase transition. *Geochim. Cosmochim. Acta.* **67**, 1991–2004.

Yapp, C.J., Poths, H., 1990. Infrared spectral evidence for a minor Fe(III) carbonate-bearing component in natural goethite. *Clay Clay Min.* **38**, 442–444.

Yapp, C.J., Poths, H., 1991. $^{13}C/^{12}C$ ratios of the Fe(III) carbonate component in natural goethites. In: Taylor, H.P.Jr., et al. (Eds.), *Stable Isotope Geochemistry: A Tribute to Samuel Epstein*. Geochem. Soc. Spec. Publ. 3, pp. 257–270.

Yapp, C.J., Poths, H., 1992. Ancient atmospheric CO_2 pressures inferred from natural goethites. *Nature* **355**, 342–344.

Yapp, C.J., Poths, H., 1993. The carbon isotope geochemistry of goethite (α-FeOOH) in ironstone of the Upper Ordovician Neda Fromation, Wisconsin, USA: implications for early Paleozoioc continental environments. *Geochim. Cosmochim. Acta.* **57**, 2599–2611.

Zeltner, W.A., Anderson, M.A., 1988. Surface charge development at the goethite/aqueous solution interface: effects of CO_2 adsorption. *Langmuir* **4**, 469–474.